AGU PUBLICATIONS

Geophysical Research Letters

RESEARCH LETTER
10.1002/2015GL066853

Key Points:
- Highest nitrous oxide production occurs at the oxic-anoxic interface
- Denitrification controls the distribution of nitrous oxide in the oxygen minimum zone
- Nitrous oxide yield increases significantly with decreasing oxygen concentrations

Supporting Information:
- Supporting Information S1

Correspondence to:
Q. Ji,
qji@princeton.edu

Citation:
Ji, Q., A. R. Babbin, A. Jayakumar, S. Oleynik, and B. B. Ward (2015), Nitrous oxide production by nitrification and denitrification in the Eastern Tropical South Pacific oxygen minimum zone, *Geophys. Res. Lett.*, *42*, 10,755–10,764, doi:10.1002/2015GL066853.

Received 2 NOV 2015
Accepted 2 DEC 2015
Accepted article online 10 DEC 2015
Published online 19 DEC 2015

Nitrous oxide production by nitrification and denitrification in the Eastern Tropical South Pacific oxygen minimum zone

Qixing Ji[1], Andrew R. Babbin[2], Amal Jayakumar[1], Sergey Oleynik[1], and Bess B. Ward[1]

[1]Department of Geosciences, Guyot Hall, Princeton University, Princeton, NJ, USA, [2]Department of Civil & Environmental Engineering, Massachusetts Institute of Technology, Cambridge, Massachusetts, USA

Abstract The Eastern Tropical South Pacific oxygen minimum zone (ETSP-OMZ) is a site of intense nitrous oxide (N_2O) flux to the atmosphere. This flux results from production of N_2O by nitrification and denitrification, but the contribution of the two processes is unknown. The rates of these pathways and their distributions were measured directly using ^{15}N tracers. The highest N_2O production rates occurred at the depth of peak N_2O concentrations at the oxic-anoxic interface above the oxygen deficient zone (ODZ) because slightly oxygenated waters allowed (1) N_2O production from both nitrification and denitrification and (2) higher nitrous oxide production yields from nitrification. Within the ODZ proper (i.e., anoxia), the only source of N_2O was denitrification (i.e., nitrite and nitrate reduction), the rates of which were reflected in the abundance of *nirS* genes (encoding nitrite reductase). Overall, denitrification was the dominant pathway contributing the N_2O production in the ETSP-OMZ.

1. Introduction

Nitrous oxide (N_2O) is important to Earth's climate because it is a strong radiation absorber and an ozone depletion agent. The recent Intergovernmental Panel on Climate Change (IPCC) report estimates that N_2O emissions to the atmosphere from the open ocean are ~3.8 Tg N yr^{-1}, ~35% of total natural emissions [*Ciais et al.*, 2013]. The highest oceanic N_2O effluxes occur in regions called oxygen minimum zones (OMZs) in the Eastern Tropical Pacific [*Cohen and Gordon*, 1978; *Arevalo-Martinez et al.*, 2015] and the Arabian Sea [*Law and Owens*, 1990; *Naqvi and Noronha*, 1991]. These OMZs are characterized by steep dissolved oxygen (O_2) gradients (oxyclines) sandwiching a layer of significant nitrite accumulation (>1 μM), which indicates anoxia ([O_2] <10 nM) [*Revsbech et al.*, 2009; *Thamdrup et al.*, 2012]. This layer of essentially zero [O_2] is referred to as the oxygen deficient zone (ODZ). At the oxic-anoxic interfaces above and below the ODZ, N_2O concentrations exceed saturation by several fold, which has presumably persisted over decades [*Babbin et al.*, 2015].

Active N_2O production is necessary for the persistence of this subsurface N_2O supersaturation. The existing gradients of inorganic nitrogen substrates and oxygen in the OMZs can support two possible microbial pathways for N_2O production, nitrification and denitrification.

Nitrification. In the presence of molecular oxygen, ammonium (NH_4^+) is oxidized to nitrite (NO_2^-) via hydroxylamine (NH_2OH) by ammonia oxidizing bacteria (AOB), with N_2O as a by-product [*Anderson*, 1964]. Ammonia oxidizing archaea (AOA) also produce N_2O by pathways that are apparently similar but less well understood [*Stieglmeier et al.*, 2014]. This nitrification-derived N_2O production pathway in marine environments has been substantiated by a positive correlation between apparent oxygen utilization and N_2O concentration excess [*Cohen and Gordon*, 1978] and by active production of $^{15}N_2O$ in ^{15}N tracer incubation experiments [*Yoshida et al.*, 1989]. Nitrification could be an especially significant source of N_2O in the OMZs because the yield of N_2O during nitrification, i.e., the ratio of N_2O production to NO_2^- production, increases dramatically with decreasing O_2 concentration as demonstrated for cultivated AOB by *Goreau et al.* [1980] and for AOA by *Löscher et al.* [2012]. These data suggest that for natural assemblages in the oxycline, the N_2O yield should increase as a result of decreasing oxygen concentration [*Codispoti and Christensen*, 1985].

Denitrification. Under anoxic and suboxic conditions ([O_2] < 10 μM), nitrate (NO_3^-) and NO_2^- can be reduced by denitrifying bacteria to N_2O through stepwise canonical denitrification. *Naqvi et al.* [2000] documented N_2O accumulation in incubation experiments and ^{15}N-N_2O production was detected in $^{15}NO_2^-$ and $^{15}NO_3^-$

tracer experiments in the Arabian Sea [*Nicholls et al.*, 2007] and the Eastern Tropical South Pacific (ETSP) OMZ [*Dalsgaard et al.*, 2012]. The series of enzymes mediating the process—nitrate reductase, nitrite reductase, nitric oxide reductase, and nitrous oxide reductase—are progressively less oxygen tolerant [*Körner and Zumft*, 1989]. Thus, under a certain oxygen concentration, reduction of NO_3^- and NO_2^- could halt at N_2O, because the reduction of N_2O to N_2 is inhibited by oxygen. This decoupling is suggested to contribute to the accumulation of N_2O by NO_3^- and NO_2^- reduction within the upper layer of the ODZ and the overlying oxycline [*Babbin et al.*, 2015]. A partial denitrification pathway is also carried out by AOB that possess the nitrite and nitric oxide reductase enzymes. AOB reduce NO_2^- to N_2O under low-oxygen conditions, a process termed "nitrifier denitrification" [*Poth and Focht*, 1985; *Frame and Casciotti*, 2010]. Nitrifier denitrification was observed in the oxygenated North Pacific subtropical gyre tracing ^{15}N transfer from NO_2^- to N_2O [*Wilson et al.*, 2014]. Characteristically, nitrifier denitrification only reduces NO_2^-, whereas both NO_3^- and NO_2^- can be utilized by denitrifiers.

In the ETSP-OMZ, NH_4^+, NO_2^-, and NO_3^- are present in the steep oxygen gradients overlying the ODZ, supporting both nitrification and denitrification. Oxygen level is probably an important factor regulating the relative contributions of nitrification and denitrification in N_2O production in OMZs [*Codispoti and Christensen*, 1985]. N_2O production rates and pathways have been modeled to estimate global fluxes using water column concentration data (e.g. *Freing et al.* [2012]). However, field studies investigating the relative contributions of different N_2O production pathways and the regulating environmental factors would be useful for (1) improving N_2O models in representing biogeochemical N_2O cycling processes in marine environments, (2) reducing the uncertainty of the magnitude of marine N_2O production rates, and (3) providing insights into future N_2O production in the ocean in response to changing climate. The present study was designed to capture the N_2O production dynamics in OMZs. Incubation experiments with ^{15}N tracers ($^{15}NH_4^+$, $^{15}NO_2^-$, and $^{15}NO_3^-$) were performed to directly measure N_2O production. Nitrification-derived N_2O production is operationally defined as $^{15}N_2O$ production from $^{15}NH_4^+$-spiked incubations. This definition focuses on the oxidative N_2O production pathways and implies the requirement for oxygen. This nitrification source potentially includes two known mechanisms by which N_2O is produced by ammonia oxidizers: N_2O produced from the hydroxylamine intermediate and N_2O produced by reduction of the NO_2^- derived from $^{15}NH_4^+$ oxidation. $^{15}N_2O$ produced in $^{15}NO_2^-$- and $^{15}NO_3^-$-spiked incubations defines the denitrification counterpart, as the reductive N_2O production pathways mediated by both nitrifiers and denitrifiers. In addition, the abundance of *nirS* genes, encoding nitrite reductase, was analyzed in relation to measured rates of NO_3^- and NO_2^- reduction to N_2O. These data could (1) determine the relative significance of nitrification compared with denitrification in N_2O production in the OMZs and (2) improve the accuracy of global marine N_2O production models by better characterizing N_2O yield during nitrification by natural assemblages rather than pure cultures in oxygenated waters where nitrification is a major pathway [*Suntharalingam and Sarmiento*, 2000; *Nevison et al.*, 2003; *Bianchi et al.*, 2012; *Zamora and Oschlies*, 2014].

2. Experiments and Methods

2.1. Study Site

Shipboard sampling and incubation were carried out on the R/V *Nathaniel B. Palmer* during June–July 2013 (NBP 1305). Samples were collected from the upper oxycline at seven transect stations and from complete depth profiles at two process stations parallel to the coast between 21.5°S and 13.0°S. Process station BB1 and BB2 represent offshore and coastal environments, respectively (Figure S1 in the supporting information).

2.2. Water Column Profiles

Water was collected in 12 L Niskin bottles mounted on a standard conductivity-temperature-depth (CTD) rosette system. An oxygen sensor (Seabird SBE43, Bellevue, WA) calibrated by Winkler titration (detection limit 2.1 μM) and a real-time STOX sensor (detection limit 10 nM; *Revsbech et al.* [2009]) were deployed on the CTD. Nutrients (NO_2^- and NO_3^-) were measured onboard using standard colorimetric protocols established by *United Nations Educational, Scientific and Cultural Organization* [1994], with detection limits of 0.02 μM. The protocol for determining NH_4^+ concentration was modified from *Mantoura and Woodward* [1983], with a detection limit of 0.01 μM. Discrete samples for N_2O concentrations were collected from Niskin bottles into acid-washed, 60 mL glass serum bottles (Wheaton, Millville, NJ) by flushing with three

volumes and sealed with a 20 mm three-prong butyl stopper (Wheaton, Millville, NJ) and an aluminum crimp seal (National Scientific, Rockwood, TN) without headspace. Within 20 min of collection, 5 mL of headspace was created with ultrahigh purity (UHP) helium (Airgas, Radnor, PA). Samples were preserved by adding 0.1 mL of saturated mercuric chloride ($HgCl_2$, Thermo Fisher Scientific, Waltham, MA) and stored in the dark until analysis.

2.3. Tracer Incubations for N_2O Production

Comprehensive N_2O production rate measurements were completed at the two process stations (Station BB1, 14.00°S, 81.20°W, bottom depth 4890 m; Station BB2, 20.50°S, 70.70°W, bottom depth 1790 m) representing offshore and coastal environments, respectively. The sampling depths were chosen to target specific water column features such as sharp [O_2] gradients and local [NO_2^-] maxima (Figures 1a and 1b). Seawater was sampled into 60 mL glass serum bottles using the same procedure described above for N_2O concentration samples (section 2.2). Headspace (5 mL) was created by replacing the volume with UHP helium. Three suites of solutions ($^{15}NH_4^+$ plus $^{14}NO_2^-$, $^{15}NO_2^-$ plus $^{14}NH_4^+$, $^{15}NO_3^-$ plus $^{14}NH_4^+$, and $^{14}NO_2^-$, 0.1 mL total volume) consisting of ^{15}N tracer (99% purity, Cambridge Isotope, Tewksbury, MA) and ^{14}N carrier (ACS grade, Thermo Fisher Scientific, Waltham, MA) were added to separate bottles in triplicate to enrich $^{15}NH_4^+$, $^{15}NO_2^-$, and $^{15}NO_3^-$ by 0.5, 1.0, and 1.0 μM (final concentration), respectively. These combinations of ^{15}N and ^{14}N solutions were designed to increase nitrogen substrate concentrations to similar levels to avoid differential stimulation of different processes. Nitrogen-15 enrichments of the initial substrate pools were usually >95%, 15–95%, and <10% for NH_4^+, NO_2^-, and NO_3^-, respectively. Tracer solutions were made from deionized water, and were degassed prior to incubation. Incubations lasted 24–36 h in a temperature-controlled environment close to (±3°C) in situ temperatures and were terminated by adding 0.1 mL of saturated $HgCl_2$ solution.

The effect of oxygen concentrations on N_2O production during nitrification and denitrification was further investigated at the upper boundary of the ODZ (80 m) at the coastal process station BB2 ([O_2] < 10 nM). Samples were acquired using a pump profiling system (PPS) equipped with a CTD package, an oxygen sensor (SBE-25, Seabird Electronics, Bellevue, WA), and a real-time STOX unit as previously described by *Canfield et al.* [2010]. The PPS minimized oxygen contamination during sampling and allowed better representation of in situ anoxic conditions during incubation experiments. After the serum bottles were filled directly from the pump outlet, sealed and 5 mL helium headspace created, volumes of 0, 0.5, and 2 mL of O_2 saturated site water (~225 μM) were injected into the sealed incubation bottles through the rubber septum to attain <0.01, 2.25, and 9 μM [O_2], concentrations representing those in the oxycline. The same suite of degassed tracers as above was utilized, and incubations lasted 24 h at in situ temperature (12°C) before termination with $HgCl_2$.

Preserved samples were stored in the dark for less than 6 months before analysis. N_2O was extracted by purging with helium for 40 min at a rate of 37 mL min^{-1} and subsequently trapped by liquid nitrogen and isolated from interference by gas chromatography. Pulses of sample N_2O were injected into an isotope ratio mass spectrometer (Delta V^{Plus}; Thermo Scientific, Waltham, MA) for mass and isotope ratio (m/z = 44, 45, 46) measurements. N_2O concentrations were calculated using the measured amount of N_2O divided by the volume of seawater (54 ± 0.4 mL). A standard curve of N_2O concentrations was generated from standard injections of 1, 2, 5, 10, 15, and 20 nmol N_2O-N into serum bottles containing 54 mL of He-flushed seawater. N_2O production from ^{15}N labeled substrate was quantified as the increase in $^{45}N_2O$ and $^{46}N_2O$ at the end of the incubation with respect to natural abundance. N_2O production rates (R_{N2O}, in nM-N d^{-1}) were calculated according to the following:

$$R_{N_2O} = \frac{[^{45}N_2O]_{t1} - [^{45}N_2O]_{t0}}{F \times \Delta t} + 2 \times \frac{[^{46}N_2O]_{t1} - [^{46}N_2O]_{t0}}{F \times \Delta t} \quad (1)$$

where $[^{45,46}N_2O]_{t1,t0}$ represent the rates of masses 45 and 46 N_2O concentration at the end (t_1) and start (t_0) of incubation. F represents the fraction of ^{15}N in the initial substrate pool (NH_4^+, NO_2^-, or NO_3^-), and Δt is incubation time. The mass spectrometer detection limit of the N_2O production is 0.005 nM d^{-1}.

2.4. Measurement of NO_2^- Production

NO_2^- production rates were measured in samples enriched with $^{15}NH_4^+$ or $^{15}NO_3^-$, using the azide reduction method [*McIlvin and Altabet*, 2005]. Seawater (5 mL) was transferred using 5 mL gas-tight glass syringe

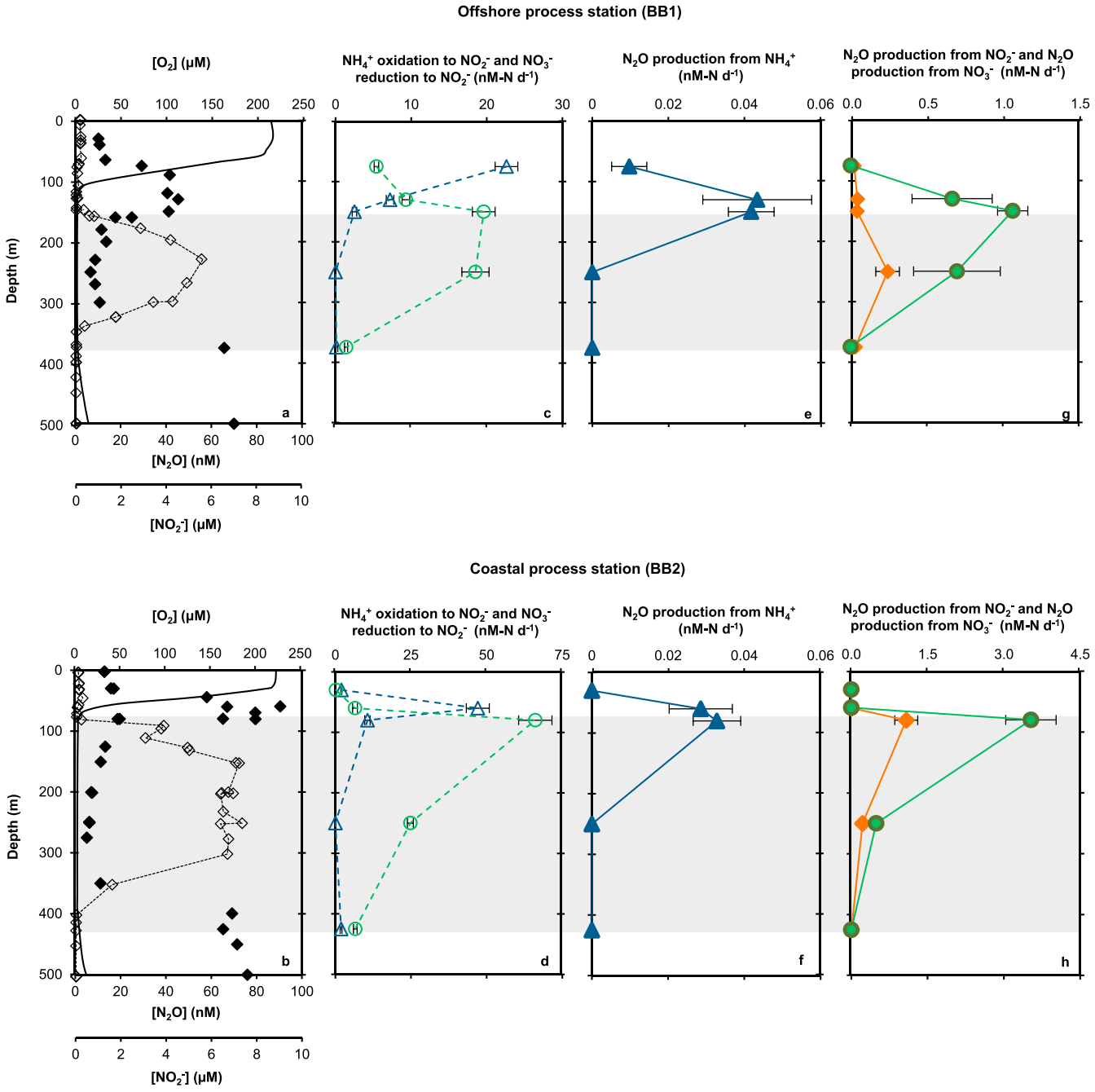

Figure 1. (a and b) Vertical concentration profiles of dissolved oxygen (solid line), N_2O (filled diamond), and NO_2^- (empty diamond with dashed line). (c and d) Rates of NH_4^+ oxidation to NO_2^- (triangles) and NO_3^- reduction to NO_2^- (circles). (e and f) Rates of N_2O production from NH_4^+ oxidation. (g and h) Rates of N_2O production from NO_2^- reduction (diamonds) and NO_3^- reduction (circles). Data from (Figures 1a, 1c, 1e, and 1g) offshore process station BB1 and (Figures 1b, 1d, 1f, and 1h) coastal process station BB2. Shaded areas represent oxygen deficient zone ($[O_2] < 10$ nM). Error bars represent standard deviation of rates determined from linear fit of time course measurements.

(Hamilton Co., Reno, NV) from serum bottles to He-flushed 20 mL vials (Grace Co., Columbia, MD). The acetic acid-treated sodium azide solution quantitatively converted NO_2^- to N_2O. The resulting N_2O was measured using a mass spectrometer as previously described. Rates were calculated as

$$R_{NO_2^-} = \frac{\left[{}^{15}NO_2^-\right]_{t1} - \left[{}^{15}NO_2^-\right]_{t0}}{F \times \Delta t} \quad (2)$$

where $[^{15}NO_2^-]_{t1,t0}$ represent $^{15}NO_2^-$ concentration at the end and start of the incubation, respectively; F represents the fraction of ^{15}N in the initial substrate pool (NH_4^+ or NO_3^-), and Δt is incubation time. The detection limit for the NO_2^- production rates is 0.01 nM d^{-1}.

N_2O production and NO_2^- production were measured in seawater incubations with $^{15}NH_4^+$ as described above. The N_2O yield was defined as the ratio of N_2O to NO_2^- production during NH_4^+ oxidation.

2.5. Water Column qPCR *nirS* Analysis

Methods of DNA extraction and qPCR for the *nirS* gene using SYBR Green have been described previously by *Jayakumar et al.* [2009, 2013]. Standardization and verification of specificity for quantitative PCR assays were performed as described in *Jayakumar et al.* [2013]. The efficiency of the qPCR reactions was calculated using the slopes of the standard curves; the efficiency ranged between 85 and 106%. The amplified products were visualized after electrophoresis in ethidium bromide stained 1.0% agarose gels and were further confirmed by cloning and sequencing the PCR product. Standards for PCR quantification of each fragment were prepared by amplifying a constructed plasmid containing the respective gene fragment, followed by quantification and serial dilution. Assays were carried out in a single assay plate [*Smith et al.*, 2006] for each gene with DNA samples (20–25 ng), from all depths in triplicates and also included no template controls, no primer control, four or more dilution of standards. DNA was quantified using PicoGreen fluorescence (Molecular Probes, Eugene, and OR) calibrated with several dilutions of phage lambda standards and qPCR was performed using a Stratagene MX3000P (Agilent Technologies, La Jolla, CA). Automatic analysis settings were used to determine the threshold cycle values. To account for DNA loss that occurs upon repeated freeze-thaw cycles, plasmid DNA and environmental DNA was quantified prior to every assay.

3. Results and Discussion

3.1. N_2O Production and Accumulation at the Oxic-Anoxic Interface

Both the offshore and coastal sampling stations were characterized by water column N_2O supersaturation at the surface (~150% saturation) and in the upper oxycline (>400% saturation), confirming that the region is important for oceanic N_2O production (Figures 1a and 1b). The peak N_2O concentrations at the oxic-anoxic interface suggest that this depth interval has unique conditions suitable for N_2O production and accumulation.

3.1.1. Ammonium Oxidation

The highest rates of NH_4^+ oxidation to NO_2^- (22–47 nM-N d^{-1}) occurred at the upper oxycline (Figures 1c and 1d) and thus contributed to the small upper (primary) NO_2^- maximum with $[NO_2^-]$ of 0.2–0.3 μM (~60 m, Figures 1a and 1b). However, the highest rates of NH_4^+ oxidation to NO_2^- did not always coincide with the highest rates of NH_4^+ oxidation to N_2O, which were detected at the peak $[N_2O]$ near the oxic-anoxic interface, with rates between 0.02 and 0.04 nM d^{-1} (Figures 1e and 1f). At the secondary nitrite maximum (SNM) where in situ $[O_2] < 10$ nM, NH_4^+ oxidation was below detection limit. Rates were low in the surface euphotic layer (30 m at station BB2) where $[NH_4^+]$ was generally high (>0.5 μM) (Figure S2).

These data from the ETSP-OMZ revealed that nitrification-derived N_2O production peaked at the oxic-anoxic interface. Fundamentally, the N_2O production rate depends on the NO_2^- production rate and is modulated by the constraints of the light, NH_4^+ availability, and O_2 distributions. The depth of the NH_4^+ oxidation rate maximum is likely the result of release from light inhibition, at a depth with adequate NH_4^+ supply and $[O_2]$, i.e., between the base of the euphotic zone and the top of the ODZ [*Codispoti and Christensen*, 1985; *Lipschultz et al.*, 1990; *Molina and Farías*, 2009]. The oxidation of NH_4^+ is inhibited by one or more factors in other depth ranges: (1) In the surface euphotic zone, nitrifiers are inhibited by light and are not competitive in NH_4^+ uptake when phytoplankton are present [*Ward*, 2005]. (2) Within the ODZ, lack of oxygen inhibits growth of nitrifiers. (3) Below the ODZ, low nitrification rates probably result from low supply of NH_4^+ [*Ward and Zafiriou*, 1988]. In addition, NH_4^+ oxidation was also detected at the top of the ODZ where in situ $[O_2] < 10$ nM (Figures 1a and 1b). This could be due to contamination by atmospheric oxygen with ~0.5 μM $[O_2]$ [*De Brabandere et al.*, 2012] during shipboard CTD sampling, but it also suggests that nitrifiers were primed to oxidize NH_4^+ at low oxygen concentrations [*Martens-Habbena et al.*, 2009].

3.1.2. Nitrite and Nitrate Reduction

The first step of denitrification, NO_3^- reduction to NO_2^-, was detected at the SNM and in the upper oxycline, with the highest rates (up to 66 nM-N d^{-1}) at the top of the ODZ. High rates of NO_3^- reduction to NO_2^- within the ODZ contributed to the accumulation of NO_2^- (up to 7 μM) and the corresponding local NO_3^- minimum (Figure S2).

The production of N_2O from denitrification (N_2O production from both NO_2^- and NO_3^- reduction) was detected within the ODZ and at the base of the oxycline at the offshore process station. At these depth intervals, over 90% of N_2O production was from denitrification, with rates of NO_2^- reduction plus NO_3^- reduction to N_2O exceeding 0.7 nM-N d^{-1}. At the oxycline below the ODZ, despite relatively high N_2O concentrations (~70 nM), N_2O production was only detected from NO_2^- reduction, at rates of ~0.02 nM d^{-1}. The experimental design cannot distinguish nitrifier denitrification from denitrifier denitrification, but the fact that N_2O production from NO_3^- usually exceeded N_2O production from NO_2^- (Figures 1g and 1h) leaves no doubt that denitrifier denitrification was the dominant process.

If both NO_3^- and NO_2^- reduction to N_2O represent denitrification, it is not clear why NO_3^- reduction rates should exceed NO_2^- reduction rates. Organic matter—the electron donor—is considered the limiting substrate for water column denitrification [*Ward et al.*, 2008; *Babbin et al.*, 2014]. The free energy gain, in terms of organic matter oxidation, under in situ conditions for NO_3^- reduction to N_2O is less thermodynamically favorable than that of NO_2^- reduction (Text S1), suggesting that NO_2^- reduction should be preferred when both NO_2^- and NO_3^- are available. However, higher rates of N_2O production from NO_3^- imply that carbon limitation may not be the main control on the reductive N_2O production. As the intermediate during denitrification, NO_2^- is able to exchange in and out of the cells [*Moir and Wood*, 2001], but the dilution of tracer with ambient $^{14}NO_2^-$ caused by this exchange should affect rates measured from $^{15}NO_3^-$ incubations. It may be that the high concentration of NO_3^- in these regions favors NO_3^- reduction by denitrifiers.

Denitrification, indicated by NO_2^- and NO_3^- reduction to N_2O was apparently not affected by $[O_2] < 10$ μM. Under manipulated $[O_2]$ between 0.01 and 9 μM, rates of NO_3^- and NO_2^- reduction to N_2O were not statistically different (Figure S3). Thus, NO_3^- and NO_2^- reduction to N_2O could occur in the oxycline overlying the ODZ, and contribute significantly to N_2O production. This is in agreement with a modeling exercise that inferred N_2O production by oxycline denitrification in the Eastern tropical North Pacific OMZ [*Babbin et al.*, 2015].

Overall, the availability of N_2O production substrates, NH_4^+, NO_2^-, and NO_3^-, coincided with suboxic conditions that allowed NH_4^+ oxidation, and NO_2^- and NO_3^- reduction to cooccur. Using the water column N_2O production rates from denitrification of 1 ± 0.25 nM-N d^{-1}, assuming the rates measured here represent average rates for OMZ regions, and that a 10 ± 4 m thick layer above the ODZ is the interval where N_2O production from denitrification exceeds consumption [*Babbin et al.*, 2015], the N_2O production from denitrification within the OMZs is estimated to be 10 ± 5 μmol of N m^{-2} d^{-1}. Assuming a layer of 75 ± 25 m above the ODZ where nitrification is contributing to N_2O production at a production rate of 0.03 ± 0.01 nM-N d^{-1}, the contribution of N_2O production from nitrification in the OMZs is 2 ± 1 μmol of N m^{-2} d^{-1}. Thus, denitrification is the major pathway of N_2O production in the OMZ regions and potentially to global marine N_2O production.

3.2. The N_2O Yield During Nitrification

The average N_2O yield was 0.04% when $[O_2]$ was close to saturation. A nonlinear increase in N_2O yield was observed at lower $[O_2]$. The yield increased significantly at $[O_2]$ below 50 μM. Samples from the top of the ODZ had higher yield (>1%); the maximum yield (1.6%) was a fortyfold increase compared to the typical yield for samples at $[O_2] > 50$ μM. Below the ODZ, N_2O production from nitrification was low to undetectable because NO_2^- production from nitrification was very slow; thus, the yield could not be determined. The direct measurement of N_2O yield (0.04–1.6%) in this study substantiated results from culture work showing a nonlinear increase in N_2O yield with decreasing in situ $[O_2]$ [*Goreau et al.*, 1980]. The majority of the ocean volume is oxygenated and nitrification is likely to dominate the N_2O source in the ocean outside the OMZs, making a considerable contribution to N_2O production on a global scale [*Dore et al.*, 1998]. Therefore, N_2O yield during nitrification is a critical parameter in estimating N_2O production from models based on nitrification and/or remineralization rates. A simple reciprocal fit to the field measurements results in a systematically

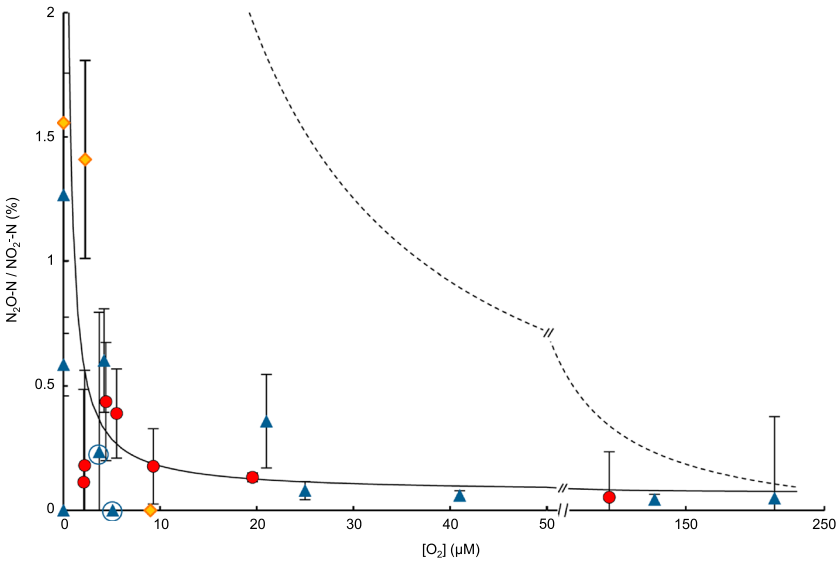

Figure 2. N_2O yield (in %), the ratio of N_2O production to NO_2^- production from NH_4^+ oxidation, measured at depths where [O_2] varied from saturation to <10 nM. Data are from upper oxycline at transect stations (circles), process stations (triangles), and [O_2] manipulation experiments (diamonds). Samples from process stations lower oxycline below the ODZ are shown as a triangle in a circle. An empirical reciprocal best fit of data (solid line) was derived for [O_2] > 10 nM: N_2O Yield (%) = 1.07/[O_2] (μM) + 0.072 and compared to the equation proposed by *Nevison et al.* [2003] (dashed line).

lower yield compared to the yield equation of *Nevison et al.* [2003], which was calibrated with data from the culture study by *Goreau et al.* [1980] (Figure 2). Therefore, global N_2O production models (e.g. *Zamora and Oschlies* [2014]; *Martinez-Rey et al.* [2015]) can be improved by incorporating field data from different oceanic basins rather than relying on culture work alone.

In addition, the N_2O yield from field measurements had a similar range to that of AOB in culture experiments and higher than that of AOA cultures (Table S1). Further research is required to investigate the relative importance of bacterial and archaeal contribution to the global marine N_2O production.

3.3. Oxygen Driven N_2O Cycling in the OMZ

The cycling of N_2O can be quantified using the N_2O residence time, i.e., the ratio of N_2O concentration to measured N_2O production rates. The calculated residence time at the surface and oxycline depths was 5.5–7 years, which was consistent with 1–10 years of water residence times in the ETSP upwelling region when mixing and advection were considered [*Johnston et al.*, 2014]. The high production rates coincided with undersaturated [N_2O] (~60% saturation) and resulted in the shortest residence times (<20 day) within the ODZ, suggesting N_2O reduction and production must be cooccuring [*Babbin et al.*, 2015]. N_2O reduction is mediated by nitrous oxide reductase (N_2OR), the most oxygen-sensitive enzyme in the denitrification pathway. N_2OR has the lowest oxygen inhibition concentration, likely at a few μM [*Bonin et al.*, 1989], whereas the enzymes nitrate reductase and nitrite reductase isolated from denitrifying bacteria had half-inhibition [O_2] of 21–25 μM. [*Körner and Zumft*, 1989]. Thus, N_2O reduction is favored within the ODZ but the activity decreases in the presence of oxygen. At the oxic-anoxic interface, this critical low, but nonzero, oxygen concentration enhances N_2O production from both nitrification and denitrification, but inhibits N_2O consumption, resulting in the characteristic N_2O peak.

Slowest N_2O production at the lower oxycline where [N_2O] was high, indicated the longest residence time (>17 years) in the water column. N_2O respiration may not be favorable likely due to low organic matter input and the presence of oxygen. Sluggish ventilation may be an important factor facilitating N_2O accumulation below the ODZ.

Due to decreased oxygen solubility by ocean warming, the marine oxygen minimum zones may potentially expand in the future [*Stramma et al.*, 2008]. Enhanced near-shore nitrogen loss rates are also possible due to increased input of anthropogenic organic matter. The resulting marine N_2O efflux is likely to increase,

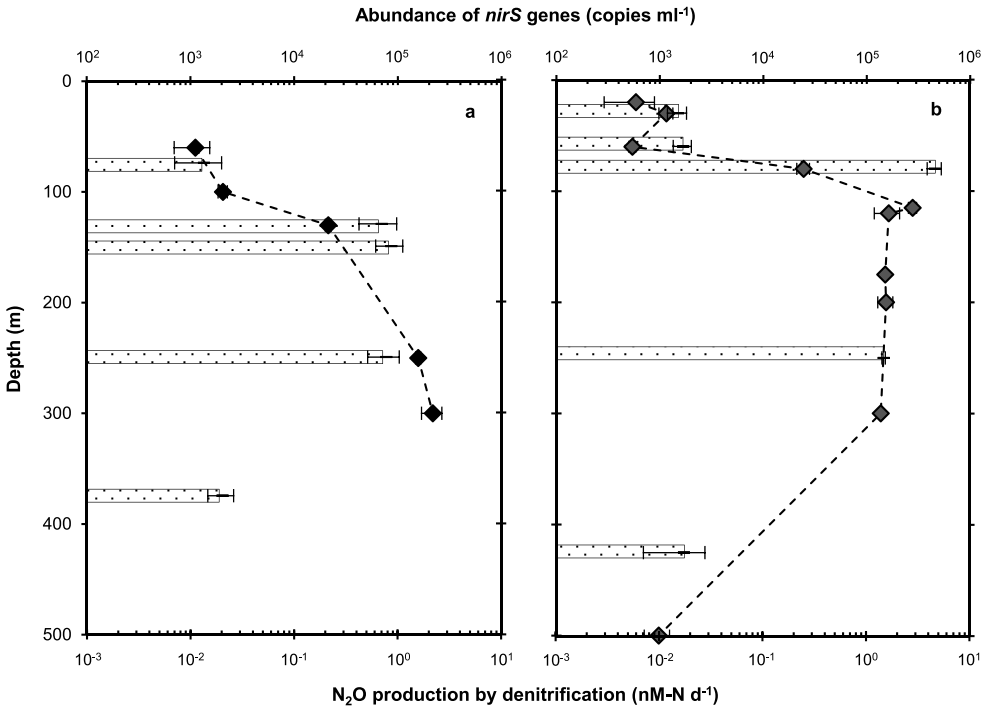

Figure 3. Distribution of *nirS* gene abundances (filled diamond with dashed line) and rates of N_2O production from denitrification (horizontal bars), defined as summation of NO_2^- and NO_3^- reduction to N_2O. Data from (a) offshore process station BB1 and (b) coastal process station BB2. Error bars on *nirS* abundances represent the standard deviation of the three replicates. The replicate values in most of the depths were so close to each other that error bars are not visible.

because (1) increase of areal coverage of low-oxygen waters enables elevated N_2O production from increasing N_2O yield from nitrification, (2) increasing temperature may enhance microbial enzymatic nitrification and denitrification at the oxic-anoxic interface and lead to enhanced N_2O production from both processes, and (3) shoaling of the upper oxycline and top of the ODZ where N_2O accumulates will increase surface N_2O supersaturation and thus increase efflux [*Codispoti*, 2010].

3.4. The *nirS* Gene as a Biomarker for Denitrifying Activity

The *nirS* gene abundance at both stations showed a gradual increase with depth and peaked within the ODZ (Figure 3). The abundance of *nirS* genes can be used as a proxy for the size of denitrifying community, assuming the *nirS* genes are present as a single copy per cell [*Zumft*, 1997]. The present analysis shows apparent covariation between the distributions of *nirS* genes and the measured N_2O production rates from denitrification (NO_2^- reduction plus NO_3^- reduction to N_2O), suggesting that the size of denitrifying community is an indicator of denitrifying activity. Low *nirS* abundances ($< 10^3$ copies mL^{-1}) were observed at the surface and the oxycline below the ODZ, indicating that *nirS*-type denitrifying bacteria were rare outside the ODZ. However, detectable NO_2^- reduction to N_2O was observed in these regions, and at this point it is not clear which genes are involved in the N_2O production processes at oxygenated depths.

4. Conclusions

The Eastern Tropical South Pacific oxygen minimum zone is a region of intense N_2O production, as indicated by surface and subsurface N_2O supersaturation, and detection of active production from nitrification and denitrification. Rates of N_2O production from denitrification are much higher than from nitrification. Denitrification is important to the production in the OMZs and by extension, global fluxes. This suggests that N_2O flux models, which identify OMZs as the major sites of pelagic N_2O emissions, could represent the biogeochemistry more accurately by incorporating both nitrification and denitrification.

Oxygen is likely an important factor regulating nitrification and denitrification in N_2O production and consumption. For nitrification-derived N_2O production, the oxycline below the euphotic zone is the

important depth range, where the N_2O yield during nitrification increases with decreasing $[O_2]$, with highest yield (>1%) at $[O_2] < 2\ \mu M$. Denitrification-derived N_2O production (NO_2^- and NO_3^- reduction to N_2O) was active under suboxic conditions, where $[O_2] < 10\ \mu M$. Therefore, at the oxic-anoxic interface, the highest N_2O production rates from both nitrification and denitrification contribute to peak N_2O concentrations in the water column. Anoxic conditions within the ODZ proper allowed a relatively large population of denitrifying bacteria to thrive, as indicated by high abundances of *nirS* genes and high rates of N_2O production from denitrification. Due to the release from oxygen inhibition, the consumption of N_2O by denitrification is more pronounced within the ODZ, such that in situ N_2O concentration is maintained at undersaturated levels. Therefore, anoxic conditions coinciding with N_2O undersaturation signal intense N_2O cycling with short turnover times leading to fixed nitrogen loss.

Acknowledgments

The authors would like to thank Calvin Mordy for providing seawater nutrient analysis, Niels Peter Revsbech for the STOX sensor data, Mark Warner for providing comparative shipboard N_2O concentration measurements, Osvaldo Ulloa and Gadiel Alarcón for the PPS operations, and Allan Devol for serving as chief scientist on R/V *Nathaniel M. Palmer*. In the preparation of the manuscript, Nicolas Van Oostende, Xuefeng Peng, and Jessica Lueders-Dumont provided valuable comments and suggestions. This research was supported by US-NSF grants to B.B.W. A.R.B. was additionally funded by a US-NSF Postdoctoral Research Fellowship in Biology (1402109). Supporting information can be found on website. The authors declare no conflict of interests.

References

Anderson, J. H. (1964), The metabolism of hydroxylamine to nitrite by Nitrosomonas, *Biochem. J.*, *91*(1), 8–17.

Arevalo-Martinez, D. L., A. Kock, C. R. Loscher, R. A. Schmitz, and H. W. Bange (2015), Massive nitrous oxide emissions from the tropical South Pacific Ocean, *Nat. Geosci.*, *8*(7), 530–533, doi:10.1038/ngeo2469.

Babbin, A. R., R. G. Keil, A. H. Devol, and B. B. Ward (2014), Organic matter stoichiometry, flux, and oxygen control nitrogen loss in the ocean, *Science*, *344*(6182), 406–408, doi:10.1126/science.1248364.

Babbin, A. R., D. Bianchi, A. Jayakumar, and B. B. Ward (2015), Rapid nitrous oxide cycling in the suboxic ocean, *Science*, *348*(6239), 1127–1129, doi:10.1126/science.aaa8380.

Bianchi, D., J. P. Dunne, J. L. Sarmiento, and E. D. Galbraith (2012), Data-based estimates of suboxia, denitrification, and N_2O production in the ocean and their sensitivities to dissolved O_2, *Global Biogeochem. Cycles*, *26*, GB2009, doi:10.1029/2011GB004209.

Bonin, P., M. Gilewicz, and J. C. Bertrand (1989), Effects of oxygen on each step of denitrification on Pseudomonas nautica, *Can. J. Microbiol.*, *35*(11), 1061–1064, doi:10.1139/m89-177.

Canfield, D. E., F. J. Stewart, B. Thamdrup, L. De Brabandere, T. Dalsgaard, E. F. Delong, N. P. Revsbech, and O. Ulloa (2010), A cryptic sulfur cycle in oxygen-minimum–zone waters off the Chilean Coast, *Science*, *330*(6009), 1375–1378, doi:10.1126/science.1196889.

Ciais, P., et al. (2013), *Carbon and Other Biogeochemical Cycles*, pp. 465–570, Cambridge Univ. Press, Cambridge, U. K., and New York.

Codispoti, L. A. (2010), Interesting times for marine N_2O, *Science*, *327*(5971), 1339–1340, doi:10.1126/science.1184945.

Codispoti, L. A., and J. P. Christensen (1985), Nitrification, denitrification and nitrous oxide cycling in the eastern tropical South Pacific ocean, *Mar. Chem.*, *16*(4), 277–300, doi:10.1016/0304-4203(85)90051-9.

Cohen, Y., and L. I. Gordon (1978), Nitrous oxide in the oxygen minimum of the eastern tropical North Pacific: Evidence for its consumption during denitrification and possible mechanisms for its production, *Deep Sea Res., Part II*, *25*(6), 509–524, doi:10.1016/0146-6291(78)90640-9.

Dalsgaard, T., B. Thamdrup, L. Farías, and N. Peter Revsbech (2012), Anammox and denitrification in the oxygen minimum zone of the eastern South Pacific, *Limnol. Oceanogr.*, *57*(5), 1331–1346, doi:10.4319/lo.2012.57.5.1331.

De Brabandere, L., B. Thamdrup, N. P. Revsbech, and R. Foadi (2012), A critical assessment of the occurrence and extend of oxygen contamination during anaerobic incubations utilizing commercially available vials, *J. Microbiol. Meth.*, *88*(1), 147–154, doi:10.1016/j.mimet.2011.11.001.

Dore, J. E., B. N. Popp, D. M. Karl, and F. J. Sansone (1998), A large source of atmospheric nitrous oxide from subtropical North Pacific surface waters, *Nature*, *396*(6706), 63–66, doi:10.1038/23921.

Frame, C. H., and K. L. Casciotti (2010), Biogeochemical controls and isotopic signatures of nitrous oxide production by a marine ammonia-oxidizing bacterium, *Biogeosciences*, *7*(9), 2695–2709, doi:10.5194/bg-7-2695-2010.

Freing, A., D. W. Wallace, and H. W. Bange (2012), Global oceanic production of nitrous oxide, *Philos. Trans. R. Soc. London B Biol. Sci.*, *367*(1593), 1245–1255, doi:10.1098/rstb.2011.0360.

Goreau, T. J., W. A. Kaplan, S. C. Wofsy, M. B. McElroy, F. W. Valois, and S. W. Watson (1980), Production of NO_2^- and N_2O by nitrifying bacteria at reduced concentrations of oxygen, *Appl. Environ. Microbiol.*, *40*(3), 526–532.

Jayakumar, A., G. D. O'Mullan, S. W. Naqvi, and B. B. Ward (2009), Denitrifying bacterial community composition changes associated with stages of denitrification in oxygen minimum zones, *Microbial Ecol.*, *58*(2), 350–362, doi:10.1007/s00248-009-9487-y.

Jayakumar, A., X. Peng, and B. Ward (2013), Community composition of bacteria involved in fixed nitrogen loss in the water column of two major oxygen minimum zones in the ocean, *Aquat. Microb. Ecol.*, *70*(3), 245–259, doi:10.3354/ame01654.

Johnston, D. T., B. C. Gill, A. Masterson, E. Beirne, K. L. Casciotti, A. N. Knapp, and W. Berelson (2014), Placing an upper limit on cryptic marine sulphur cycling, *Nature*, *513*(7519), 530–533, doi:10.1038/nature13698.

Körner, H., and W. G. Zumft (1989), Expression of denitrification enzymes in response to the dissolved oxygen level and respiratory substrate in continuous culture of Pseudomonas stutzeri, *Appl. Environ. Microbiol.*, *55*(7), 1670–1676.

Law, C. S., and N. J. P. Owens (1990), Significant flux of atmospheric nitrous oxide from the northwest Indian Ocean, *Nature*, *346*(6287), 826–828.

Lipschultz, F., S. C. Wofsy, B. B. Ward, L. A. Codispoti, G. Friedrich, and J. W. Elkins (1990), Bacterial transformations of inorganic nitrogen in the oxygen-deficient waters of the Eastern Tropical South Pacific Ocean, *Deep Sea Res., Part I*, *37*(10), 1513–1541, doi:10.1016/0198-0149(90)90060-9.

Löscher, C. R., A. Kock, M. Könneke, J. LaRoche, H. W. Bange, and R. A. Schmitz (2012), Production of oceanic nitrous oxide by ammonia-oxidizing archaea, *Biogeosciences*, *9*(7), 2419–2429, doi:10.5194/bg-9-2419-2012.

Mantoura, R. F. C., and E. M. S. Woodward (1983), Optimization of the indophenol blue method for the automated determination of ammonia in estuarine waters, *Estuarine Coastal Shelf Sci.*, *17*(2), 219–224, doi:10.1016/0272-7714(83)90067-7.

Martens-Habbena, W., P. M. Berube, H. Urakawa, J. R. de la Torre, and D. A. Stahl (2009), Ammonia oxidation kinetics determine niche separation of nitrifying archaea and bacteria, *Nature*, *461*(7266), 976–979, doi:10.1038/nature08465.

Martinez-Rey, J., L. Bopp, M. Gehlen, A. Tagliabue, and N. Gruber (2015), Projections of oceanic N_2O emissions in the 21st century using the IPSL Earth system model, *Biogeosciences*, *12*(13), 4133–4148, doi:10.5194/bg-12-4133-2015.

McIlvin, M. R., and M. A. Altabet (2005), Chemical conversion of nitrate and nitrite to nitrous oxide for nitrogen and oxygen isotopic analysis in freshwater and seawater, *Anal. Chem.*, *77*(17), 5589–5595.

Moir, J. W. B., and N. J. Wood (2001), Nitrate and nitrite transport in bacteria, *Cell. Mol. Life Sci.*, *58*(2), 215–224, doi:10.1007/PL00000849.

Molina, V., and L. Farías (2009), Aerobic ammonium oxidation in the oxycline and oxygen minimum zone of the eastern tropical South Pacific off northern Chile (~20°S), *Deep Sea Res., Part II*, *56*(16), 1032–1041, doi:10.1016/j.dsr2.2008.09.006.

Naqvi, S. W. A., and R. J. Noronha (1991), Nitrous oxide in the Arabian Sea, *Deep Sea Res., Part I*, *38*(7), 871–890, doi:10.1016/0198-0149(91)90023-9.

Naqvi, S. W. A., D. A. Jayakumar, P. V. Narvekar, H. Naik, V. V. S. S. Sarma, W. D'Souza, S. Joseph, and M. D. George (2000), Increased marine production of N_2O due to intensifying anoxia on the Indian continental shelf, *Nature*, *408*(6810), 346–349, doi:10.1038/35042551.

Nevison, C., J. H. Butler, and J. W. Elkins (2003), Global distribution of N_2O and the ΔN_2O-AOU yield in the subsurface ocean, *Global Biogeochem. Cycles*, *17*(4), 1119, doi:10.1029/2003GB002068.

Nicholls, J. C., C. A. Davies, and M. Trimmer (2007), High-resolution profiles and nitrogen isotope tracing reveal a dominant source of nitrous oxide and multiple pathways of nitrogen gas formation in the central Arabian Sea, *Limnol. Oceanogr.*, *52*(1), 156–168, doi:10.2307/40006070.

Poth, M., and D. D. Focht (1985), (15)N kinetic analysis of N(2)O production by Nitrosomonas europaea: An examination of nitrifier denitrification, *Appl. Environ. Microbiol.*, *49*(5), 1134–1141.

Revsbech, N. P., L. H. Larsen, J. Gundersen, T. Dalsgaard, O. Ulloa, and B. Thamdrup (2009), Determination of ultra-low oxygen concentrations in oxygen minimum zones by the STOX sensor, *Limnol. Oceanogr. Methods*, *7*, 371–381.

Smith, C. J., D. B. Nedwell, L. F. Dong, and A. M. Osborn (2006), Evaluation of quantitative polymerase chain reaction-based approaches for determining gene copy and gene transcript numbers in environmental samples, *Environ. Microbiol.*, *8*(5), 804–815.

Stieglmeier, M., M. Mooshammer, B. Kitzler, W. Wanek, S. Zechmeister-Boltenstern, A. Richter, and C. Schleper (2014), Aerobic nitrous oxide production through N-nitrosating hybrid formation in ammonia-oxidizing archaea, *ISME J.*, *8*(5), 1135–1146, doi:10.1038/ismej.2013.220.

Stramma, L., G. C. Johnson, J. Sprintall, and V. Mohrholz (2008), Expanding oxygen-minimum zones in the tropical oceans, *Science*, *320*(5876), 655–658, doi:10.1126/science.1153847.

Suntharalingam, P., and J. L. Sarmiento (2000), Factors governing the oceanic nitrous oxide distribution: Simulations with an ocean general circulation model, *Global Biogeochem. Cycles*, *14*(1), 429–454, doi:10.1029/1999GB900032.

Thamdrup, B., T. Dalsgaard, and N. P. Revsbech (2012), Widespread functional anoxia in the oxygen minimum zone of the Eastern South Pacific, *Deep Sea Res., Part I*, *65*, 36–45, doi:10.1016/j.dsr.2012.03.001.

United Nations Educational, Scientific and Cultural Organization (1994), *Protocols for the Joint Global Ocean Flux Study (JGOFS) Core Measurements*, edited by I. O. Commission, United Nations Educational, Scientific and Cultural Organization.

Ward, B. B. (2005), Temporal variability in nitrification rates and related biogeochemical factors in Monterey Bay, California, USA, *Mar. Ecol. Prog. Ser.*, *292*, 97–109, doi:10.3354/meps292097.

Ward, B. B., and O. C. Zafiriou (1988), Nitrification and nitric oxide in the oxygen minimum of the eastern tropical North Pacific, *Deep Sea Res., Part A*, *35*(7), 1127–1142, doi:10.1016/0198-0149(88)90005-2.

Ward, B. B., C. B. Tuit, A. Jayakumar, J. J. Rich, J. Moffett, and S. W. A. Naqvi (2008), Organic carbon, and not copper, controls denitrification in oxygen minimum zones of the ocean, *Deep Sea Res., Part I*, *55*(12), 1672–1683, doi:10.1016/j.dsr.2008.07.005.

Wilson, S. T., D. A. del Valle, M. Segura-Noguera, and D. M. Karl (2014), A role for nitrite in the production of nitrous oxide in the lower euphotic zone of the oligotrophic North Pacific Ocean, *Deep Sea Res., Part I*, *85*, 47–55, doi:10.1016/j.dsr.2013.11.008.

Yoshida, N., H. Morimoto, M. Hirano, I. Koike, S. Matsuo, E. Wada, T. Saino, and A. Hattori (1989), Nitrification rates and ^{15}N abundances of N_2O and NO_3^- in the western North Pacific, *Nature*, *342*(6252), 895–897, doi:10.1038/342895a0.

Zamora, L. M., and A. Oschlies (2014), Surface nitrification: A major uncertainty in marine N_2O emissions, *Geophys. Res. Lett.*, *41*, 4247–4253, doi:10.1002/2014GL060556.

Zumft, W. G. (1997), Cell biology and molecular basis of denitrification, *Microbiol. Mol. Biol. Rev.*, *61*(4), 533–616.